JACS
JOURNAL OF THE AMERICAN CHEMICAL SOCIETY
pubs.acs.org/JACS
Article

Combined Theoretical and Experimental Studies Unravel Multiple Pathways to Convergent Asymmetric Hydrogenation of Enamides

Jianping Yang,[⊥] Luca Massaro,[⊥] Suppachai Krajangsri, Thishana Singh, Hao Su, Emanuele Silvi, Sudipta Ponra, Lars Eriksson, Mårten S. G. Ahlquist, and Pher G. Andersson*

Cite This: J. Am. Chem. Soc. 2021, 143, 21594−21603
Read Online
ACCESS | Metrics & More | Article Recommendations | Supporting Information

ABSTRACT: We present a highly efficient convergent asymmetric hydrogenation of *E*/*Z* mixtures of enamides catalyzed by N,P−iridium complexes supported by mechanistic studies. It was found that reduction of the olefinic isomers (*E* and *Z* geometries) produces chiral amides with the same absolute configuration (enantioconvergent hydrogenation). This allowed the hydrogenation of a wide range of *E*/*Z* mixtures of trisubstituted enamides with excellent enantioselectivity (up to 99% *ee*). A detailed mechanistic study using deuterium labeling and kinetic experiments revealed two different pathways for the observed enantioconvergence. For α-aryl enamides, fast isomerization of the double bond takes place, and the overall process results in kinetic resolution of the two isomers. For α-alkyl enamides, no double bond isomerization is detected, and competition experiments suggested that substrate chelation is responsible for the enantioconvergent stereochemical outcome. DFT calculations were performed to predict the correct absolute configuration of the products and strengthen the proposed mechanism of the iridium-catalyzed isomerization pathway.

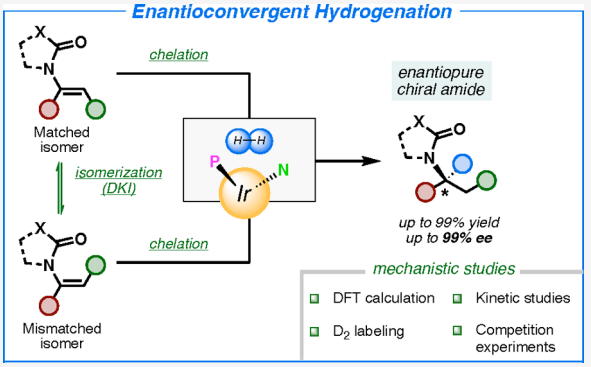

INTRODUCTION

The asymmetric hydrogenation of prochiral olefins is one of the most practical and efficient transformations for the preparation of enantiopure compounds.[1] A wide number of Rh(I), Ru(II), and Ir(I) catalytic systems have been extensively studied and applied to diversely functionalized olefins.[2]

Despite the successful results and considerable mechanistic understanding in this field, several challenges still remain. In the asymmetric hydrogenation of trisubstituted olefins, the *E* and *Z* geometries of the substrate generally produce opposite enantiomers of the products (Scheme 1a, divergent hydrogenation).[3] This limits the possibility of achieving high stereoselectivity in the reduction of isomeric mixtures, which leads to a difficult and time-consuming purification of the olefinic substrates. Therefore, catalytic systems that can directly hydrogenate *E*/*Z* mixtures to yield enantiomerically pure products are highly desired. Unfortunately, only a few catalysts have been reported to efficiently transform both *E* and *Z* isomers into the same enantiomer of the product with equally high enantioselectivity (Scheme 1b, convergent hydrogenation). From a mechanistic point, the literature reports several proposals that are used to rationalize the stereochemical outcome of the hydrogenation, especially for catalytic systems having rhodium, ruthenium, and iridium complexes.[4] Detailed mechanistic insight is required to identify what clearly distinguishes these two opposite enantioselective behaviors (divergence and convergence) and to understand whether the differences lie in the catalyst properties or the nature of the substrates. The divergent outcome has been rationalized and demonstrated in several cases.[4c,5] However, to the best of our knowledge, studies to elucidate the enantioconvergent outcome have rarely been reported.[2a]

Historically, enamides have received much attention as strategic starting materials to synthesize valuable chiral amines.[6] The limitation of many of the reported methodologies is related to the geometry of the starting materials (Scheme 1a).[3b,h,7] An exception is the hydrogenation of multifunctionalized enamides, such as α-dehydroamino acids, using Rh−DuPHOS catalysts, which reduced the *E* and *Z* isomers to the same enantiopure products (Scheme 1b).[8] Recent catalytic systems based on BINAPO−Ru and Ni−Binapine also showed excellent convergence for the hydrogenation of amino acid precursors.[9] Mechanistic studies on these systems excluded the presence of double-bond isomerization, but in-depth mechanistic studies were not presented.

Received: September 10, 2021
Published: December 14, 2021

https://doi.org/10.1021/jacs.1c09573
J. Am. Chem. Soc. 2021, 143, 21594−21603

Scheme 1. Enantiodivergent and Enantioconvergent Hydrogenation

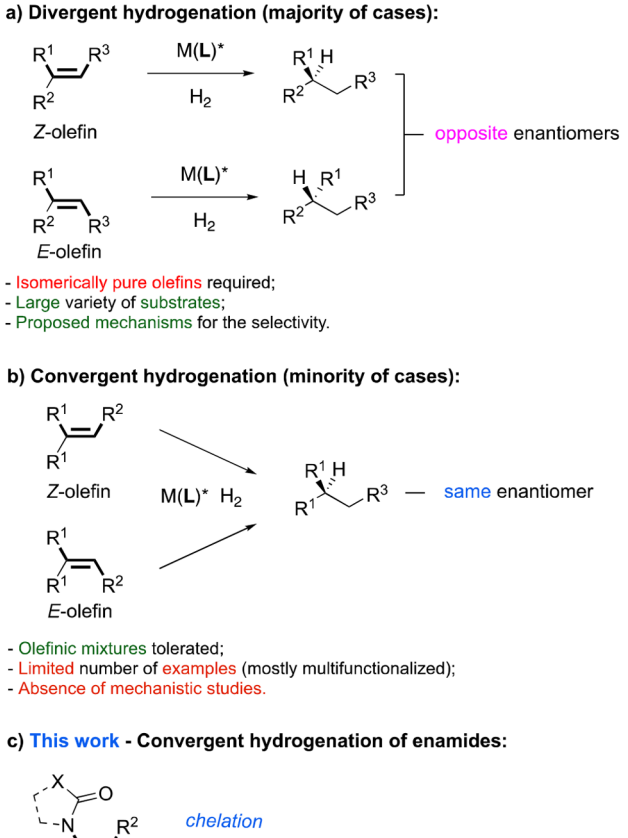

We decided to investigate the asymmetric hydrogenation of simple trisubstituted enamides with our N,P−iridium complexes, since this class of catalysts have often shown a strong dependence on the double-bond geometry. During the optimization of the reaction conditions, we surprisingly found that both the *E* and *Z* isomers were converted to the same enantiomer with high optical purity (Scheme 1c). Intrigued by these enantioconvergent results, we examined four different classes of enamides, defined by different geometric and electronic properties (Figure 1). Each class was evaluated against a large number of substrates, and in-depth mechanistic studies were carried out to elucidate the origin of this unusual selectivity. The optimized results and catalyst structures for each class are presented in Table 2 and Scheme 7.

RESULTS AND DISCUSSION

Mechanistic Investigation. *Class 1.* The *E* and *Z* isomers of *α,β*-diphenyl-substituted enamide **1a** were used as model

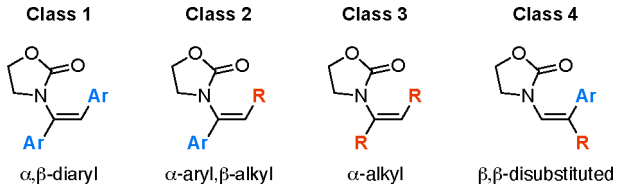

Figure 1. Classes of enamides.

substrates for class 1 (Scheme 2). Under the optimized reaction conditions (for optimization details, see Tables S1–S5), both the *E* and *Z* isomers of **1a** gave the *R* enantiomer with high selectivity (96% and 93% *ee*, respectively). To shed light on the enantioselective outcome of this transformation, hydrogenations were performed using D_2 gas (Scheme 3). We

Scheme 2. Hydrogenation of Class 1 Enamides

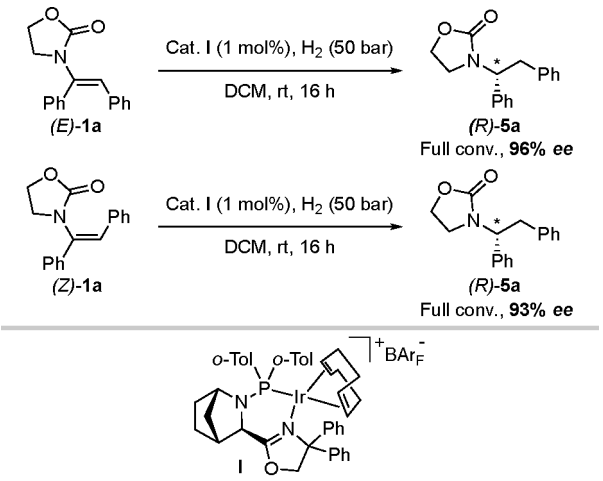

Scheme 3. Deuterium Labeling Experiments for Class 1

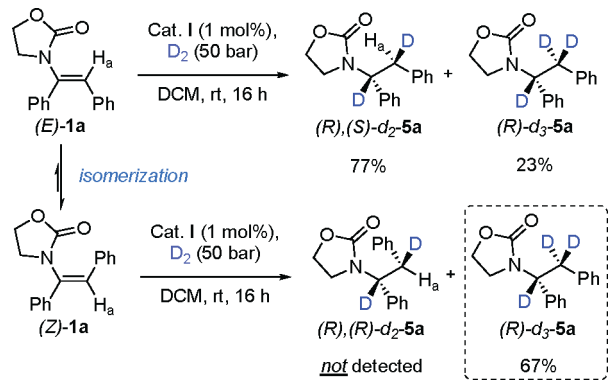

hypothesized that a stereospecific cis addition of D_2 to the *E* and *Z* enamide carbon−carbon double bond would generate a pair of diastereomeric products unless isomerization occurs, which would instead result in the formation of a single diastereomer.[10] The *E* isomer was examined first and gave full conversion to the expected deuterated product d_2-**5a**, showing the signal of proton H_a as a singlet at 3.34 ppm (Figure 2a; the complete spectrum is given in Figure S2). However, the *Z* isomer surprisingly resulted in trideuterated d_3-**5a** as the major product. The signal of the benzylic proton H_a disappeared because H_a was completely exchanged with a deuterium atom,

https://doi.org/10.1021/jacs.1c09573
J. Am. Chem. Soc. 2021, 143, 21594−21603

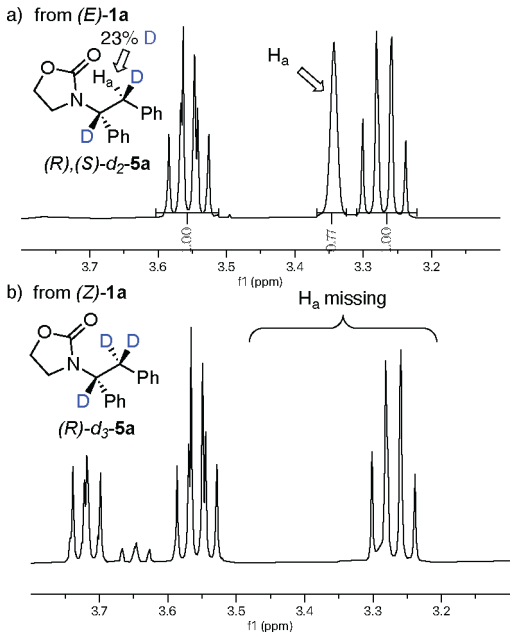

Figure 2. ^{1}H NMR spectra for the deuterium experiments. (a) For (*E*)-**1a**, H_a of the product at δ 3.34 integrates to 0.77. (b) (*Z*)-**1a** shows the presence of product d_3-**5a** without the benzylic proton. The **5a**/*Z*/*E* ratio is 12:5:1.

and in addition, some remaining starting material (*Z* isomer) and the formation of the *E* isomer were detected from the residual oxazolidinone peaks (Figure 2b). These results could be explained by an isomerization of the double bond in which the catalyst exchanges the vinylic hydrogen with a deuterium atom.[11] Next, we investigated the kinetic profile for the hydrogenation of the two isomers (*E*)-**1a** and (*Z*)-**1a** (Figure 3). In both cases, the formation of the other isomer could be detected by NMR spectroscopy *before* complete conversion to the reduced products. Moreover, thermodynamic equilibrium between the two isomers of the starting material was achieved in less than 60 min.[12] The reaction starting from the *E* isomer gave a 69% yield of the product **5a**, while the one starting from the *Z* isomer produced only a 40% yield of the hydrogenated product over 1 h. In both cases the isomeric ratio of **1a** in the remaining reaction mixture was in favor of the thermodynamically more stable but less reactive *Z* isomer. This is also in agreement with the deuterium experiment, in which (*Z*)-**1a** is not hydrogenated directly but instead undergoes an isomerization involving the complete exchange of the benzylic proton (Figure 3 and Table S6).

These data suggest that the reduced product is generated via the less abundant diastereoisomer present in the reaction (the *E* isomer).[13] The thermodynamically stable but slow-reacting *Z* isomer instead isomerizes to the fast-reacting *E* isomer via reversible migratory insertion/β-hydride elimination and is consequently hydrogenated. DFT calculations for the asymmetric hydrogenation of the two isomers and for the isomerization process were carried out to support this assumption (Figure 4). The dihydride species $\mathbf{I_{DH}}$ (Figure 4, center) is the starting point for all of the reactions.[14] We considered various starting geometries in which the iridium dihydride coordinates exclusively to the enamide double bond (Figure S6), but these complexes resulted in much higher energies than the chelated species, where both the carbonyl group and the double bond are coordinated. Moreover, chelation trans to nitrogen resulted in the most reasonable energies, which is in agreement with previously reported studies of the hydrogenation of functionalized olefins.[15] The calculated pathways with the lowest energy are presented for both (*Z*)-**1a** (Figures 4, left, and S7) and (*E*)-**1a** (Figures 4, right, and S8). The migratory insertion barrier revealed a ΔE of ~2 kcal mol^{-1} in favor of the *E* isomer ($\mathbf{TS_{Z1-2}}$ vs $\mathbf{TS_{E1-2}}$; Figure S9). The catalytic cycles then continue with coordination of a new dihydrogen molecule to form the respective intermediates **Z3** and **E3**. To conclude, σ-complex-assisted metathesis releases the respective products in the rate-determining step. Here as well, the ΔE barrier favors the *E* isomer route (~2.3 kcal mol^{-1}; Figure S9), which generates product **5a** with the correct *R* configuration in agreement with the experimental results. Interestingly, the two favored mechanistic pathways related to the *E* and *Z* geometries would lead, as often reported, to opposite enantiomers.[3] The convergent outcome is enabled by an isomerization and involves another migratory insertion step in which the iridium atom coordinates to the more hindered prochiral carbon of the *Z* isomer (**Iso2**; Figure 4, bottom). Notably, this process is almost barrierless ($\mathbf{TS_{Iso1-2}}$, 0.09 kcal mol^{-1}). Rotation of the C−C single bond followed by β-hydride elimination ($\mathbf{TS_{Iso3-4}}$) forms the *E* isomer. The energy barrier for the described steps is lower than 13 kcal mol^{-1}, suggesting that this process is

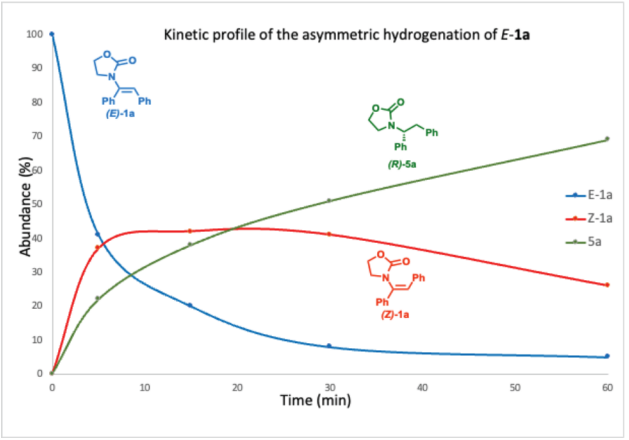

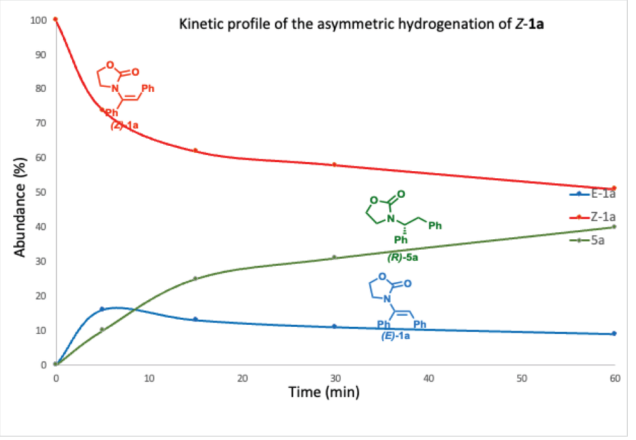

Figure 3. Kinetic profiles for hydrogenation of (a) *E*-**1a** and (b) *Z*-**1a**.

https://doi.org/10.1021/jacs.1c09573
J. Am. Chem. Soc. 2021, 143, 21594−21603

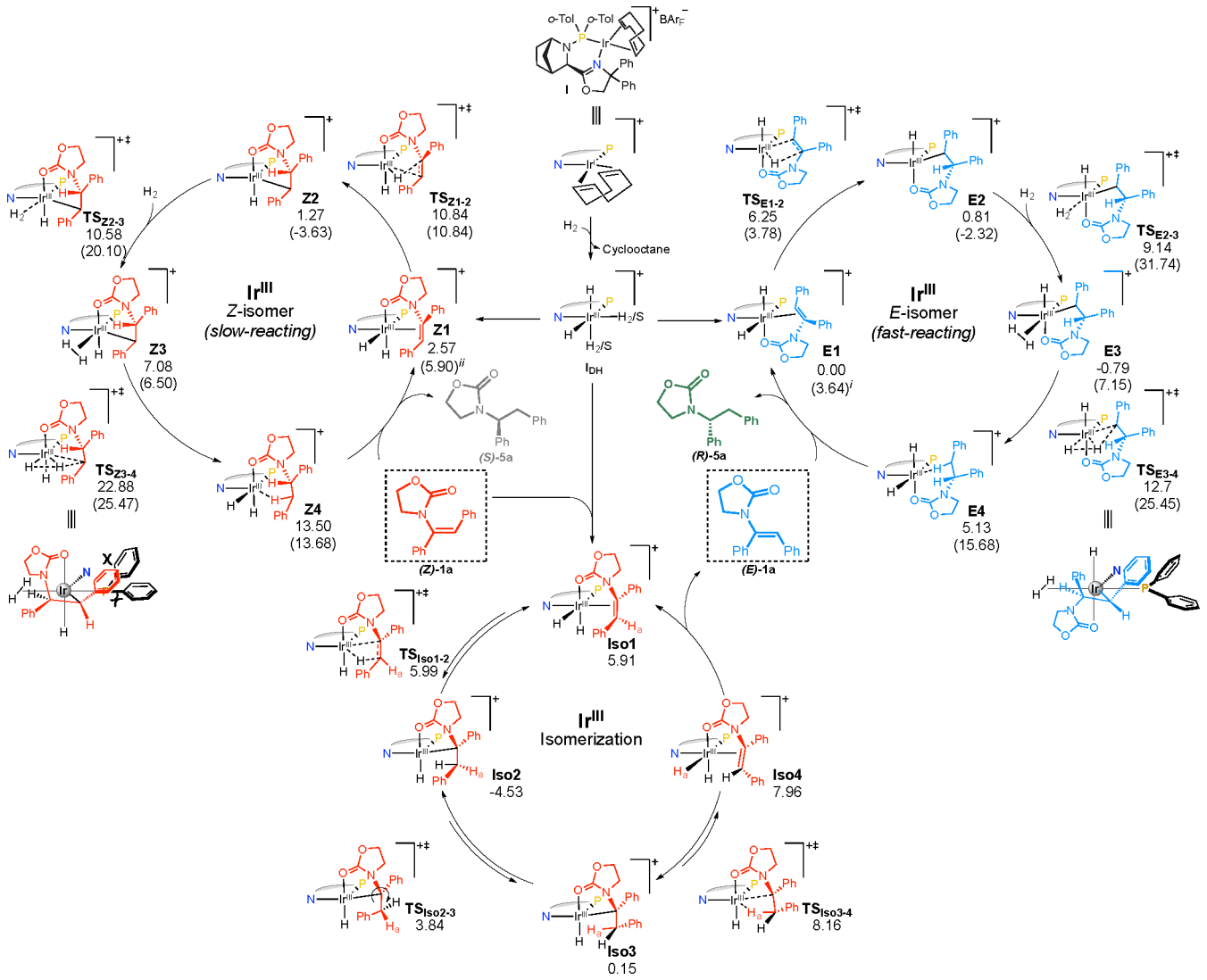

Figure 4. DFT-calculated free energy profile for the hydrogenation of class 1 enamides: (right) *E* isomer; (left) *Z* isomer; (bottom) reversible isomerization pathway. [i]The free energy of the pathway toward the *S* configuration is shown in parentheses. [ii]The free energy of the pathway toward the *R* configuration is shown in parentheses.

faster than the hydrogenation rate-determining step ($\Delta G_{TS_{Z3-4}-Z3}$ = 15.8 kcal mol^{-1} and $\Delta G_{TS_{E3-4}-E3}$ = 13.49 kcal mol^{-1}; Figure S9). These calculations correspond with the experimental results, supporting the iridium-catalyzed dynamic isomerization as the mechanistic reason for the enantioconvergent hydrogenation and confirming the presence of fast- and slow-reacting isomers.

Class 2. We then turned our attention to the second class of enamides, which have an aliphatic chain as the *β*-substituent (Table 1). The hydrogenation of the *E* and *Z* isomers of compound **2a** using the standard reaction conditions and thiazole-based catalyst **II** yielded considerably different results. While the *Z* isomer gave 99% *ee* favoring the *R* enantiomer (Table 1, entry 1), the *E* isomer had a modest *ee* of 38% with the opposite configuration (Table 1, entry 2). Intrigued by these results, we re-evaluated the reaction conditions, which revealed that the stereochemical outcome of the reaction is strongly dependent on both the temperature and the hydrogen pressure (Table S4). Indeed, with 1 bar H_2 and an increased temperature of 60 °C, the enantioselective outcome for *E* isomer of **2a** shifted to favor the *R* enantiomer with 80% *ee*

Table 1. Class 2 Optimization of Enantioconvergence[a]

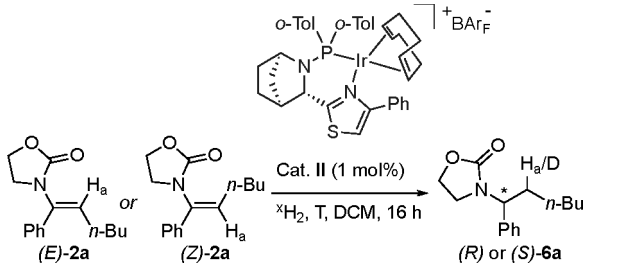

entry	isomer	H_2 or D_2 pressure (bar)	temp.	conv.	*ee* (%)	H_a/D exchange (%)
1	*Z*	50	rt	full	99 (*R*)	<5
2	*E*	50	rt	full	38 (*S*)	<5
3[b]	*Z*	1	60 °C	full	97 (*R*)	<5
4[b]	*E*	1	60 °C	95%	80 (*R*)	42

[a]Reaction conditions: 0.05 mmol of substrates in 0.5 mL of DCM. Hydrogenation and deuterium labeling studies were carried out following the same protocol. [b]Dichloroethane was used as the solvent.

https://doi.org/10.1021/jacs.1c09573
J. Am. Chem. Soc. 2021, 143, 21594−21603

(Table 1, entry 4). For the *Z* isomer of **2a**, these reaction conditions had a negligible effect, since the change was from 99% to 97% *ee* in favor of the *R* enantiomer (Table 1, entry 3). The enantioconvergent results obtained using the new reaction conditions are in accordance with the proposed mechanism for class 1 enamides, as the elevated temperature increases the rate of the isomerization process and the lower hydrogen pressure retards the hydrogenation.[4b] We began deuterium experiments on the *E* and *Z* isomers of **2a** using a pressure of 50 bar at room temperature (Figure S3). However, when the modified reaction conditions were used (i.e., higher temperature and lower pressure), deuterium exchange occurred, resembling that of the class 1 enamides. Here, the *E* isomer showed deuterium exchange of H_a (Table 1, entry 4), while the *Z* isomer was completely converted to product d_2-**6a** and no proton exchange was detected (Table 1, entry 3, and Figure S4).

These data suggest an enantiodivergent outcome at room temperature, which can be changed by the use of low pressure and high temperature, favoring the isomerization of the *E* isomer to the *Z* isomer and resulting in an enantioconvergent reaction (Scheme 4, low *P* and high *T*).

Scheme 4. Hydrogenation Pathways for Class 2 Enamides[a]

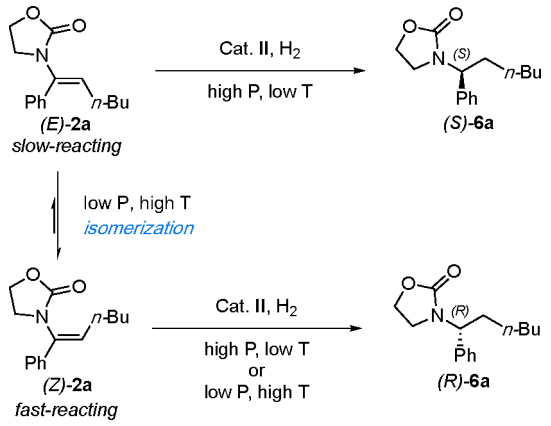

[a]The enantioselective outcome for (*E*)-**2a** is dependent on the H_2 pressure and the temperature. Low pressure and high temperature favor the isomerization toward (Z)-**2a**, enabling an enantioconvergent hydrogenation.

Class 3. Enamides **3a** of class 3, which bear an aliphatic moiety at the α-position and a phenyl substituent at the β-position, were also investigated (Scheme 5). For this class, the *E* and *Z* stereoisomers again afforded convergent results under the standard reaction conditions as described for class 1. Proline-based catalyst **III**[16] gave the highest enantioselectivity for the hydrogenation of both (*E*)-**3a** and (*Z*)-**3a** (94% and 95% *ee*, respectively) and products having the same absolute configuration. Deuterium experiments indicated an absence of isomerization for both the *E* and *Z* isomers (Scheme 6 and Figure 5). A 1:1 *E*/*Z* mixture was also hydrogenated using D_2 gas and produced an equal diastereomeric mixture of 1:1 (Figure S5).

This class of enamides, even without isomerization, achieved a high level of convergent stereoselectivity. A possible explanation for this is that the chelation-controlled hydrogenation for both the *E* and *Z* isomers leads to the same enantiomer of the product. As mentioned earlier, this is a rather uncommon observation in asymmetric hydrogenations,

Scheme 5. Hydrogenation of Class 3 Enamides

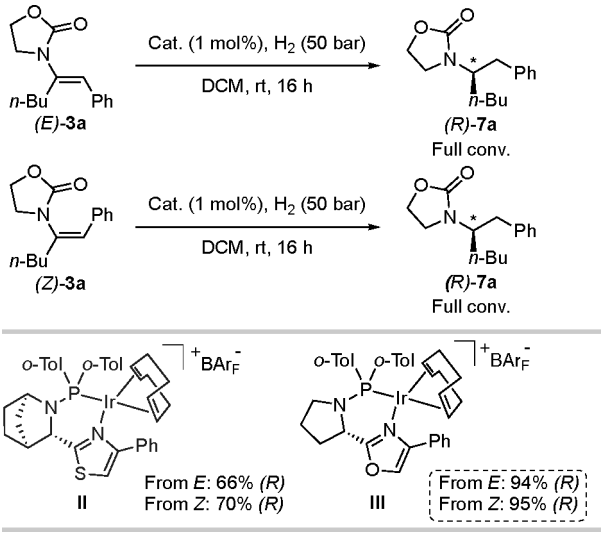

Scheme 6. Deuterium Labeling Experiments for Class 3

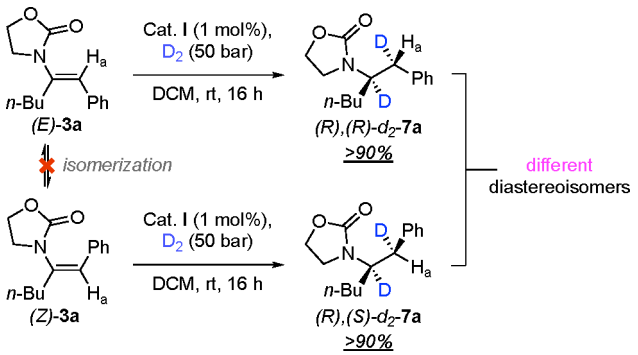

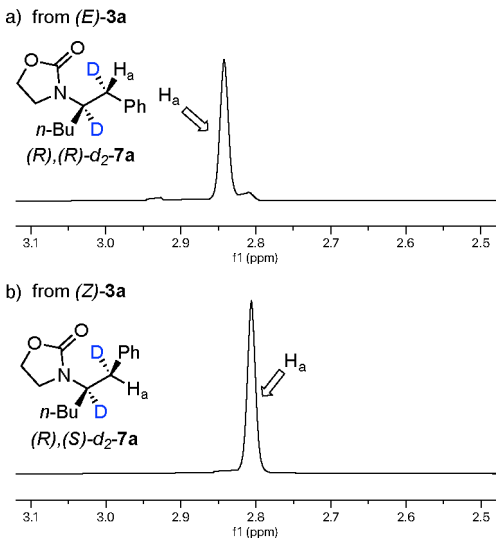

Figure 5. ^{1}H NMR spectra for the deuterium experiments (a) from (*E*)-**3a** and (b) from (*Z*)-**3a**. The two diastereoisomers can be clearly distinguished thanks to the H_a signal.

and to get further support for it, DFT calculations were carried out (Figures S11 and S12). Interestingly, when class 3 substrate **3b** was subjected to DFT calculations, it was found that both the *E* and *Z* isomers resulted in low-energy pathways that produce the same and correct *R* enantiomer.

https://doi.org/10.1021/jacs.1c09573
J. Am. Chem. Soc. 2021, 143, 21594−21603

Class 4. Finally, the β,β-disubstituted enamides (class 4) were evaluated (Scheme 7). When the two isomers of

Scheme 7. Divergent Hydrogenation of *E* and *Z* Isomers of Class 4 Enamides[a]

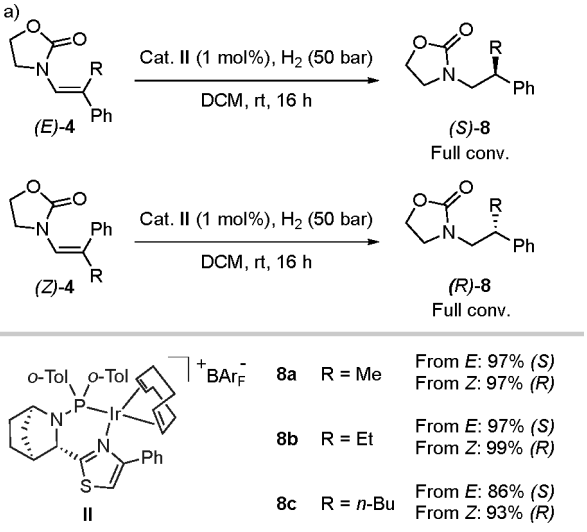

[a]Reaction conditions: 0.1 mmol of substrates in 1 mL of DCM. Conversion was determined by ^{1}H NMR spectroscopy. Enantiomeric excess was determined by supercritical fluid chromatography (SFC) analysis using chiral stationary phases.

compound **4a** were hydrogenated, the resulting products indicated that an enantiodivergent mechanism was followed. The selectivity for the *E* isomer was 97% *ee* in favor of the *S* product, whereas the *Z* isomer selectivity was 97% *ee* favoring the *R* product. The same trend was observed for substrates with longer alkyl chains, producing the opposite enantiomers for products **8b** and **8c** with good selectivity. For this class of enamides, the chelating group binds to the non-prochiral carbon, which precludes them from undergoing the same isomerization that is operative for classes 1 and 2.

Chelation Effect. As mentioned above, the different classes can undergo convergent hydrogenation either because of isomerization toward the fast-reacting isomer or simply because the *E* and *Z* isomers are reduced to the same enantiomer with favorable energies. Regardless of these mechanistic differences, DFT calculations performed for classes 1 and 3 unanimously showed that the carbonyl coordinates to iridium in the hydrogenation process (see Figure 4 for class 1 and Figures S11 and S12 for class 3). This observation is in stark contrast with the mechanism normally associated with asymmetric hydrogenation of olefins using N,P−iridium complexes. We hypothesized that chelation of the amide group would result in a chemoselective hydrogenation of the enamide in the presence of a simple olefin. A competition experiment was carried out in which an equimolar mixture of *trans*-methylstilbene (*E*)-**9** and enamide (*E*)-**3b** was subjected to hydrogenation (Scheme 8). The reaction was monitored over time, and it was found that the enamide was consumed over 9 h and that no conversion of **9** was observed *before* **3b** had been consumed (Figure 6a). Interestingly, the independent hydrogenation of *trans*-methylstilbene with N,P−iridium complex **III** showed a reversed order of reactivity, with more than 60% conversion in 2 h (Figure 6b) versus 35%

Scheme 8. Competition Experiments

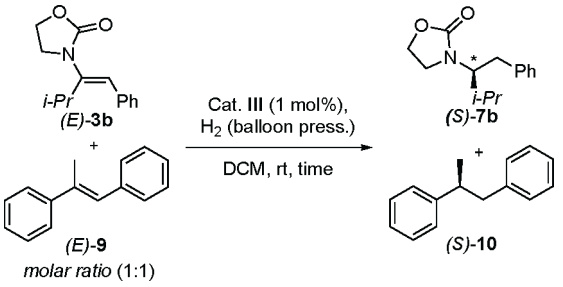

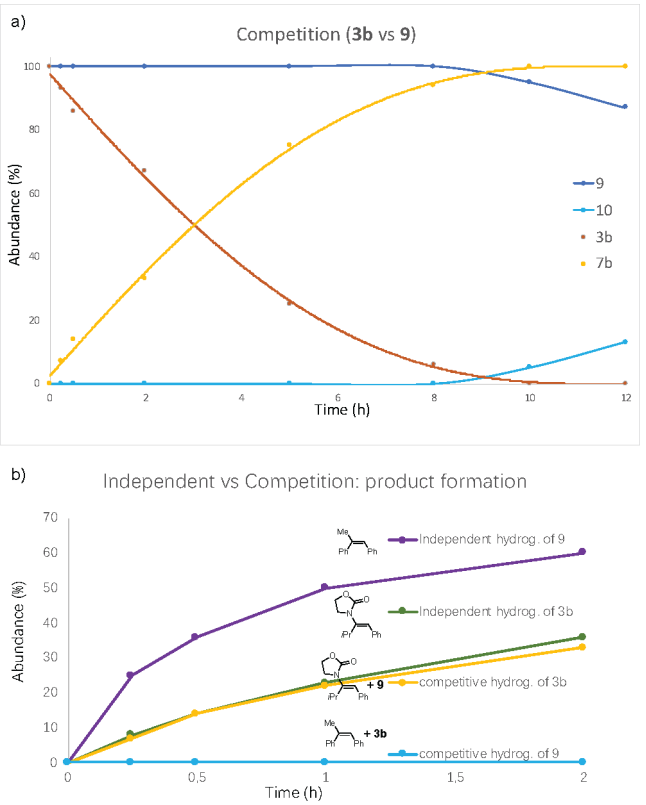

Figure 6. (a) Kinetic profiles for the competition experiment between enamide (*E*)-**3b** and methylstilbene (*E*)-**9**. (b) Kinetic profiles for independent and competitive hydrogenation of (*E*)-**3b** and (*E*)-**9**.

conversion of the amide. The same competition experiment was also performed for hydrogenation of class 1 enamides and resulted in the same outcome (Figure S1).

Substrate Scope. To show the usefulness of the enantioconvergent hydrogenation, a wide scope of *E*/*Z* mixtures of enamides belonging to each class was evaluated (Table 2). Class 1 substrates were hydrogenated as 2:1 *E*/*Z* mixtures using the standard conditions (50 bar, room temperature) (Table 2). Different substituents on the α-phenyl ring were well-tolerated. Products **5b** and **5c** bearing a *p*-chloro and *p*-methyl group, respectively, were obtained with excellent enantioselectivity and isolated yield. Interestingly, enamides **1d** with a *p*-methoxy group and **1e** with a *p*-trifluoromethyl group showed lower reactivity. However, it was possible to attain full conversion in excellent yield and enantioselectivity using the modified reaction conditions suitable for class 2, favoring the isomerization of the extremely unreactive *Z* isomer of these two compounds. Also, products bearing heteroaromatic groups were tested (Table 2, **5f** and

https://doi.org/10.1021/jacs.1c09573
J. Am. Chem. Soc. 2021, 143, 21594−21603

Table 2. Substrate Scope

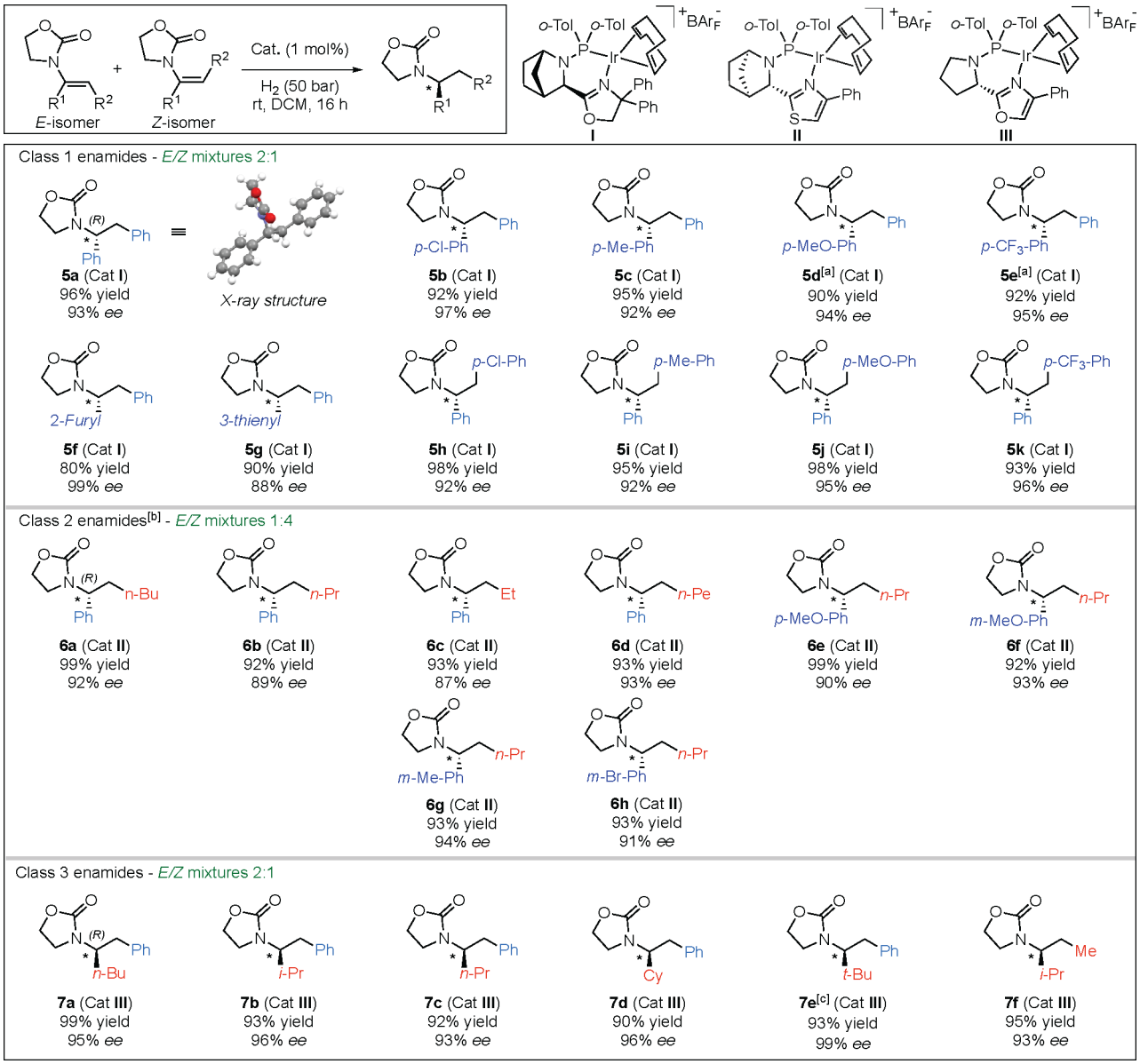

[a]Reaction conditions: 0.15 mmol of substrate, 1 mol % catalyst, and 1.5 mL of DCM. Conversion was determined by ^{1}H NMR spectroscopy. Enantiomeric excess was determined by SFC or GC analysis using chiral stationary phases. [b]Class 2 optimized conditions: H_2 (1 bar) at 60 °C in 1 mL of DCE. [c]A 9:1 *E*/*Z* mixture was employed.

Table 3. Scope of Amide Groups[a]

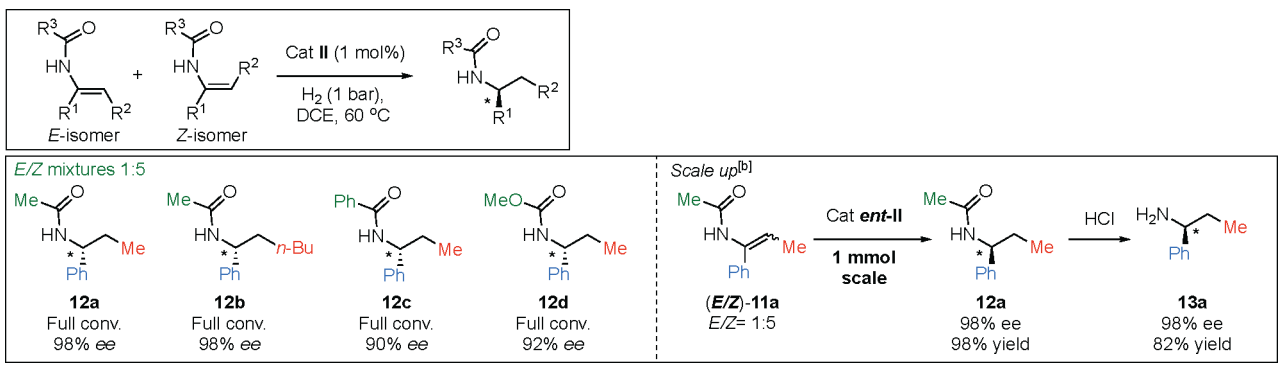

[a]Reaction conditions: 0.05 mmol of substrate, 1 mol % catalyst, 0.5 mL of DCE. [b]1 mmol of substrate, 1 mol % catalyst, 2 mL of DCE.

https://doi.org/10.1021/jacs.1c09573
J. Am. Chem. Soc. 2021, 143, 21594−21603

5g) and showed behavior similar to those with aromatic rings. Gratifyingly, the 2-furyl group showed very high selectivity. Next, we evaluated different substituents on the β-phenyl ring, which gave products in high yields with high selectivity (over 92% *ee*) in all cases (Table 2, **5h**−**k**). We continued with class 2 using the optimized conditions for isomeric mixtures (Table 1, entries 3 and 4) and a 1:4 *Z*/*E* isomer ratio, which can be easily obtained from a recent protocol developed in our laboratory.[17] Different aliphatic linear chains (butyl, propyl, ethyl, and pentyl) were tested, and all gave good selectivity and excellent yields (Table 2, **6a**−**d**).

We then tested different substituents on the aromatic ring and obtained the best results for the methoxy and methyl electron-donating groups. The enamide having bromine at the meta position also gave **6h** with an *ee* and yield higher than 90%. The enamides of class 3 were evaluated using the novel optimized catalyst **III** (Table 2). No isomerization was observed for these substrates, but stereochemical convergence was still achieved, probably as a result of chelation-controlled hydrogenation. The hydrogenation of a 2:1 *E*/*Z* mixture of enamide **3a** bearing the *n*-butyl chain resulted in an excellent 95% *ee* of product **7a**, and similar results were obtained for isopropyl, *n*-propyl, and cyclohexyl (**7b**, **7c**, and **7d**, respectively). When the aliphatic moiety was changed to the more hindered *tert*-butyl group, the conversion was lower, but the thermodynamic 9:1 *E*/*Z* mixture gave an excellent 99% *ee* and 93% yield (Table 2, **7e**)

To further improve the usefulness in synthesis, different amides that are easier to deprotect were also evaluated (Table 3).[18] Products with the acetamide group (**12a** and **12b**) were obtained with an almost perfect selectivity of 98% *ee*. The benzamide group and the methyl carbamate (**12c** and **12d**) were also tolerated, giving 90% and 92% *ee*, respectively. Finally, when the hydrogenation of the *E*/*Z* mixture of enamide **11a** was scaled up, the high selectivity of 98% *ee* was retained, and the subsequent deprotection of the acetyl group furnished chiral amine **13a** in good yield.

CONCLUSIONS

We have developed a new and efficient asymmetric hydrogenation of trisubstituted linear enamides using N,P−iridium catalysts. These catalytic systems successfully hydrogenated a wide range of differently substituted mixtures of *E* and *Z* isomers with excellent enantioselectivities. This is an uncommon feature for N,P−iridium catalysts, since the majority of reported proposed mechanisms involve a stereoselectivity-determining step based on steric discrimination of the non-prochiral carbon of the double bond. Furthermore, we have revealed the presence of at least two different mechanistic pathways for the enantioconvergent hydrogenation of enamides: via isomerization and via chelation control. These mechanisms are strongly influenced by the stereoelectronic properties of the substrates, and division of the enamides into classes helped to rationalize the different results.

Finally, DFT studies were carried out to understand the enantioconvergent routes for the hydrogenation of chelating olefins, and they predicted the correct absolute configuration and the fast isomerization of the *E* and *Z* isomers.

ASSOCIATED CONTENT

Supporting Information

The Supporting Information is available free of charge at https://pubs.acs.org/doi/10.1021/jacs.1c09573.

Experimental procedures, additional experimental details, full spectroscopic data for all new compounds, and computational details with Cartesian coordinates of optimized structures (PDF)

Accession Codes

CCDC 1955080 contains the supplementary crystallographic data for this paper. These data can be obtained free of charge via www.ccdc.cam.ac.uk/data_request/cif, or by emailing data_request@ccdc.cam.ac.uk, or by contacting The Cambridge Crystallographic Data Centre, 12 Union Road, Cambridge CB2 1EZ, U.K.; fax: +44 1223 336033.

AUTHOR INFORMATION

Corresponding Author

Pher G. Andersson − *Department of Organic Chemistry, Stockholm University, 106 91 Stockholm, Sweden; School of Chemistry and Physics, University of Kwazulu-Natal, Durban 4000, South Africa;* orcid.org/0000-0002-1383-8246; Email: Pher.Andersson@su.se

Authors

Jianping Yang − *Department of Organic Chemistry, Stockholm University, 106 91 Stockholm, Sweden;* orcid.org/0000-0001-8431-6368

Luca Massaro − *Department of Organic Chemistry, Stockholm University, 106 91 Stockholm, Sweden;* orcid.org/0000-0001-6806-6039

Suppachai Krajangsri − *Department of Organic Chemistry, Stockholm University, 106 91 Stockholm, Sweden*

Thishana Singh − *School of Chemistry and Physics, University of Kwazulu-Natal, Durban 4000, South Africa*

Hao Su − *School of Biotechnology, KTH Royal Institute of Technology, 106 91 Stockholm, Sweden;* orcid.org/0000-0002-0178-6610

Emanuele Silvi − *Department of Organic Chemistry, Stockholm University, 106 91 Stockholm, Sweden*

Sudipta Ponra − *Department of Organic Chemistry, Stockholm University, 106 91 Stockholm, Sweden*

Lars Eriksson − *Department of Materials and Environmental Chemistry, Stockholm University, 106 91 Stockholm, Sweden*

Mårten S. G. Ahlquist − *School of Biotechnology, KTH Royal Institute of Technology, 106 91 Stockholm, Sweden;* orcid.org/0000-0002-1553-4027

Complete contact information is available at: https://pubs.acs.org/10.1021/jacs.1c09573

Author Contributions

[⊥]J.Y. and L.M. contributed equally.

Notes

The authors declare no competing financial interest.

ACKNOWLEDGMENTS

We thank the University of Camerino, School of Science and Technology, Chemistry Division, for the collaboration through the Erasmus+ Program. The Swedish Research Council (VR), Stiftelsen Olle Engkvist Byggmästare, and the Knut and Alice Wallenberg Foundation (KAW 2016.0072 and KAW 2018:0066) supported this work. T.S. acknowledges the NRF South Africa for the Post-PhD Track Thuthuka Grant. All of the calculations were performed on resources provided by the Swedish National Infrastructure for Computing (SNIC) at PDC Centre for High Performance Computing (PDC-HPC)

through the project "Small Molecule Activation by Transition Metals in Complex Environments" (SNIC 2020/6-47) and the National Supercomputing Center in Linköping, Sweden (Projects SNIC 2019/3-6 and SNIC 2020/6-47).

REFERENCES

(1) (a) Wen, J.; Wang, F.; Zhang, X. Asymmetric hydrogenation catalyzed by first-row transition metal complexes. *Chem. Soc. Rev.* **2021**, *50* (5), 3211−3237. (b) Seo, C. S.; Morris, R. H. Catalytic homogeneous asymmetric hydrogenation: successes and opportunities. *Organometallics* **2019**, *38* (1), 47−65. (c) Margarita, C.; Andersson, P. G. Evolution and prospects of the asymmetric hydrogenation of unfunctionalized olefins. *J. Am. Chem. Soc.* **2017**, *139* (4), 1346−1356. (d) Chirik, P. J. Iron-and cobalt-catalyzed alkene hydrogenation: catalysis with both redox-active and strong field ligands. *Acc. Chem. Res.* **2015**, *48* (6), 1687−1695. (e) Minnaard, A. J.; Feringa, B. L.; Lefort, L.; De Vries, J. G. Asymmetric hydrogenation using monodentate phosphoramidite ligands. *Acc. Chem. Res.* **2007**, *40* (12), 1267−1277. (f) Cui, X.; Burgess, K. Catalytic homogeneous asymmetric hydrogenations of largely unfunctionalized alkenes. *Chem. Rev.* **2005**, *105* (9), 3272−3296.

(2) (a) Massaro, L.; Zheng, J.; Margarita, C.; Andersson, P. G. Enantioconvergent and enantiodivergent catalytic hydrogenation of isomeric olefins. *Chem. Soc. Rev.* **2020**, *49* (8), 2504−2522. (b) Zhu, S.-F.; Zhou, Q.-L. Iridium-catalyzed asymmetric hydrogenation of unsaturated carboxylic acids. *Acc. Chem. Res.* **2017**, *50* (4), 988−1001. (c) Verendel, J. J.; Pamies, O.; Dieguez, M.; Andersson, P. G. Asymmetric hydrogenation of olefins using chiral crabtree-type catalysts: scope and limitations. *Chem. Rev.* **2014**, *114* (4), 2130−2169. (d) Etayo, P.; Vidal-Ferran, A. Rhodium-catalysed asymmetric hydrogenation as a valuable synthetic tool for the preparation of chiral drugs. *Chem. Soc. Rev.* **2013**, *42* (2), 728−754. (e) Roseblade, S. J.; Pfaltz, A. Iridium-catalyzed asymmetric hydrogenation of olefins. *Acc. Chem. Res.* **2007**, *40* (12), 1402−1411. (f) Genet, J.-P. Asymmetric catalytic hydrogenation. Design of new Ru catalysts and chiral ligands: from laboratory to industrial applications. *Acc. Chem. Res.* **2003**, *36* (12), 908−918. (g) Zhang, Z.; Butt, N. A.; Zhang, W. Asymmetric Hydrogenation of Nonaromatic Cyclic Substrates. *Chem. Rev.* **2016**, *116* (23), 14769−14827. (h) Xie, J.-H.; Zhu, S.-F.; Zhou, Q.-L. Recent advances in transition metal-catalyzed enantioselective hydrogenation of unprotected enamines. *Chem. Soc. Rev.* **2012**, *41* (11), 4126−4139. (i) Wang, D.-S.; Chen, Q.-A.; Lu, S.-M.; Zhou, Y.-G. Asymmetric hydrogenation of heteroarenes and arenes. *Chem. Rev.* **2012**, *112* (4), 2557−2590. (j) Yuan, Q.; Liu, D.; Zhang, W. Iridium-Catalyzed Asymmetric hydrogenation of β,γ-unsaturated γ-Lactams: scope and mechanistic studies. *Org. Lett.* **2017**, *19* (5), 1144−1147.

(3) (a) Yan, Q.; Xiao, G.; Wang, Y.; Zi, G.; Zhang, Z.; Hou, G. Highly efficient enantioselective synthesis of chiral sulfones by Rh-catalyzed asymmetric hydrogenation. *J. Am. Chem. Soc.* **2019**, *141* (4), 1749−1756. (b) Zhang, J.; Liu, C.; Wang, X.; Chen, J.; Zhang, Z.; Zhang, W. Rhodium-catalyzed asymmetric hydrogenation of β-branched enamides for the synthesis of β-stereogenic amines. *Chem. Commun.* **2018**, *54* (47), 6024−6027. (c) Liu, G.; Han, Z.; Dong, X.-Q.; Zhang, X. Rh-catalyzed asymmetric hydrogenation of β-substituted-β-thio-α,β-unsaturated esters: Expeditious access to chiral organic sulfides. *Org. Lett.* **2018**, *20* (18), 5636−5639. (d) Peters, B. K.; Zhou, T.; Rujirawanich, J.; Cadu, A.; Singh, T.; Rabten, W.; Kerdphon, S.; Andersson, P. G. An enantioselective approach to the preparation of chiral sulfones by Ir-catalyzed asymmetric hydrogenation. *J. Am. Chem. Soc.* **2014**, *136* (47), 16557−16562. (e) Wang, A.; Wüstenberg, B.; Pfaltz, A. Enantio-and diastereoselective hydrogenation of farnesol and O-protected derivatives: stereocontrol by changing the C=C bond configuration. *Angew. Chem.* **2008**, *120* (12), 2330−2332. (f) Powell, M. T.; Hou, D.-R.; Perry, M. C.; Cui, X.; Burgess, K. Chiral imidazolylidine ligands for asymmetric hydrogenation of aryl alkenes. *J. Am. Chem. Soc.* **2001**, *123* (36), 8878−8879. (g) Takaya, H.; Ohta, T.; Sayo, N.; Kumobayashi, H.; Akutagawa, S.; Inoue, S.; Kasahara, I.; Noyori, R. Enantioselective hydrogenation of allylic and homoallylic alcohols. *J. Am. Chem. Soc.* **1987**, *109* (5), 1596−1597. (h) Miyashita, a. A.; Yasuda, A.; Takaya, H.; Toriumi, K.; Ito, T.; Souchi, T.; Noyori, R. Synthesis of 2,2′-bis(diphenylphosphino)-1,1′-binaphthyl (BINAP), an atropisomeric chiral bis(triaryl)phosphine, and its use in the rhodium(I)-catalyzed asymmetric hydrogenation of α-(acylamino)acrylic acids. *J. Am. Chem. Soc.* **1980**, *102* (27), 7932−7934.

(4) (a) Li, W.; Wagener, T.; Hellmann, L.; Daniliuc, C. G.; Mück-Lichtenfeld, C.; Neugebauer, J.; Glorius, F. Design of Ru(II)-NHC-Diamine precatalysts directed by ligand cooperation: applications and mechanistic investigations for asymmetric hydrogenation. *J. Am. Chem. Soc.* **2020**, *142* (15), 7100−7107. (b) Gridnev, I. D.; Liu, Y.; Imamoto, T. Mechanism of asymmetric hydrogenation of β-Dehydroamino acids catalyzed by rhodium complexes: large-scale experimental and computational study. *ACS Catal.* **2014**, *4* (1), 203−219. (c) Church, T. L.; Rasmussen, T.; Andersson, P. G. Enantioselectivity in the iridium-catalyzed hydrogenation of unfunctionalized olefins. *Organometallics* **2010**, *29* (24), 6769−6781. (d) Brandt, P.; Hedberg, C.; Andersson, P. G. New mechanistic insights into the iridium−phosphanooxazoline-catalyzed hydrogenation of unfunctionalized olefins: a DFT and kinetic study. *Chem. - Eur. J.* **2003**, *9* (1), 339−347. (e) Halpern, J. Mechanism and stereoselectivity of asymmetric hydrogenation. *Science* **1982**, *217* (4558), 401−407. (f) Chan, A.; Pluth, J.; Halpern, J. Identification of the enantioselective step in the asymmetric catalytic hydrogenation of a prochiral olefin. *J. Am. Chem. Soc.* **1980**, *102* (18), 5952−5954.

(5) Mazuela, J.; Norrby, P.-O.; Andersson, P. G.; Pamies, O.; Dieguez, M. Pyranoside phosphite−oxazoline ligands for the highly versatile and enantioselective Ir-catalyzed hydrogenation of minimally functionalized olefins. a combined theoretical and experimental study. *J. Am. Chem. Soc.* **2011**, *133* (34), 13634−13645.

(6) (a) Ponra, S.; Boudet, B.; Phansavath, P.; Ratovelomanana-Vidal, V. Recent developments in transition-metal-catalyzed asymmetric hydrogenation of enamides. *Synthesis* **2021**, *53* (2), 193−214. (b) Xie, J.-H.; Zhu, S.-F.; Zhou, Q.-L. Transition metal-catalyzed enantioselective hydrogenation of enamines and imines. *Chem. Rev.* **2011**, *111* (3), 1713−1760.

(7) (a) Doherty, S.; Smyth, C. H.; Harriman, A.; Harrington, R. W.; Clegg, W. Can a butadiene-based architecture compete with its biaryl counterpart in asymmetric catalysis? Enantiopure Me-CATPHOS, a remarkably efficient ligand for asymmetric hydrogenation. *Organometallics* **2009**, *28* (3), 888−895. (b) Fukatsu, K.; Uchikawa, O.; Kawada, M.; Yamano, T.; Yamashita, M.; Kato, K.; Hirai, K.; Hinuma, S.; Miyamoto, M.; Ohkawa, S. Synthesis of a novel series of benzocycloalkene derivatives as melatonin receptor agonists. *J. Med. Chem.* **2002**, *45* (19), 4212−4221. (c) Kagan, H. B.; Dang, T.-P. Asymmetric catalytic reduction with transition metal complexes. I. Catalytic system of rhodium(I) with (−)-2,3-*O*-isopropylidene-2,3-dihydroxy-1,4-bis(diphenylphosphino)butane, a new chiral diphosphine. *J. Am. Chem. Soc.* **1972**, *94* (18), 6429−6433.

(8) Burk, M. J.; Feaster, J. E.; Nugent, W. A.; Harlow, R. L. Preparation and use of C_2-symmetric bis(phospholanes): production of α-amino acid derivatives via highly enantioselective hydrogenation reactions. *J. Am. Chem. Soc.* **1993**, *115* (22), 10125−10138.

(9) (a) Long, J.; Gao, W.; Guan, Y.; Lv, H.; Zhang, X. Nickel-catalyzed highly enantioselective hydrogenation of β-acetylamino vinylsulfones: access to chiral β-amido sulfones. *Org. Lett.* **2018**, *20* (18), 5914−5917. (b) Zhou, Y.-G.; Tang, W.; Wang, W.-B.; Li, W.; Zhang, X. Highly effective chiral ortho-substituted BINAPO ligands (o-BINAPO): Applications in Ru-catalyzed asymmetric hydrogenations of β-aryl-substituted β-(acylamino) acrylates and β-keto esters. *J. Am. Chem. Soc.* **2002**, *124* (18), 4952−4953.

(10) Koenig, K. E.; Knowles, W. S. Use of deuterium to investigate *E-Z* isomerizations during rhodium-catalyzed reduction. Asymmetric induction and mechanistic implications. *J. Am. Chem. Soc.* **1978**, *100* (24), 7561−7564.

(11) Another possible explanation for the isomerization of the double bond is the acidity of the reaction mixture, which is generated by the acidic character of the iridium catalysts and is the key property

https://doi.org/10.1021/jacs.1c09573
J. Am. Chem. Soc. 2021, 143, 21594−21603

to enable several reactions. To confirm this hypothesis, the *E* and *Z* isomers of enamide **1a** were analyzed using different acids in DCM. Beginning with the pure *E* isomer, the isomerization was monitored and found to progress slowly toward the thermodynamic equilibrium of 6:1 *Z*/*E* (usually over 1 week; see Table S7). Also, when the iridium hydride complex (generated from catalyst **I** and a stoichiometric amount of H_2) was used as the acid source, it resulted in similar rates of isomerization. For the acidic character of the iridium catalysts, see: (a) Krajangsri, S.; Wu, H.; Liu, J.; Rabten, W.; Singh, T.; Andersson, P. G. Tandem Peterson olefination and chemoselective asymmetric hydrogenation of *β*-hydroxy silanes. *Chem. Sci.* **2019**, *10* (12), 3649−3653. (b) Liu, J.; Krajangsri, S.; Yang, J.; Li, J.-Q.; Andersson, P. G. Iridium-catalysed asymmetric hydrogenation of allylic alcohols via dynamic kinetic resolution. *Nat. Catal.* **2018**, *1* (6), 438−443. (c) Zhu, Y.; Fan, Y.; Burgess, K. Carbene-metal hydrides can be much less acidic than phosphine-metal hydrides: significance in hydrogenations. *J. Am. Chem. Soc.* **2010**, *132* (17), 6249−6253.

(12) These reaction rates are significantly different from those for the isomerization in an acidic medium (1 h vs 1 week), which indicates that a different mechanistic pathway than the Brønsted acid-catalyzed isomerization must be operational.

(13) For a discussion of the major/minor principle, see: (a) Schmidt, T.; Dai, Z.; Drexler, H. J.; Hapke, M.; Preetz, A.; Heller, D. The major/minor concept: dependence of the selectivity of homogeneously catalyzed reactions on reactivity ratio and concentration ratio of the intermediates. *Chem. - Asian J.* **2008**, *3* (7), 1170−1180. (b) Landis, C. R.; Halpern, J. Asymmetric hydrogenation of methyl (*Z*)-*α*-acetamidocinnamate catalyzed by [1,2-bis(phenyl-*o*-anisoyl)-phosphino)ethane]rhodium(I): kinetics, mechanism and origin of enantioselection. *J. Am. Chem. Soc.* **1987**, *109* (6), 1746−1754.

(14) Mazet, C.; Smidt, S. P.; Meuwly, M.; Pfaltz, A. A combined experimental and computational study of dihydrido-(phosphinooxazoline)iridium complexes. *J. Am. Chem. Soc.* **2004**, *126* (43), 14176−14181.

(15) (a) Li, M.-L.; Yang, S.; Su, X.-C.; Wu, H.-L.; Yang, L.-L.; Zhu, S.-F.; Zhou, Q.-L. Mechanism studies of Ir-catalyzed asymmetric hydrogenation of unsaturated carboxylic acids. *J. Am. Chem. Soc.* **2017**, *139* (1), 541−547. (b) Engel, J.; Mersmann, S.; Norrby, P. O.; Bolm, C. Mechanistic insights into the iridium-catalyzed hydrogenations of *α*, *β*-unsaturated ketones. *ChemCatChem* **2016**, *8* (19), 3099−3106. (c) Liu, Y.; Gridnev, I. D.; Zhang, W. Mechanism of the asymmetric hydrogenation of exocyclic *α*,*β*-unsaturated carbonyl compounds with an Iridium/BiphPhox catalyst: NMR and DFT studies. *Angew. Chem.* **2014**, *126* (7), 1932−1936.

(16) Diéguez, M.; Mazuela, J.; Pàmies, O.; Verendel, J. J.; Andersson, P. G. Chiral pyranoside Phosphite-Oxazolines: a new class of ligand for asymmetric catalytic hydrogenation of alkenes. *J. Am. Chem. Soc.* **2008**, *130* (23), 7208−7209.

(17) Massaro, L.; Yang, J.; Krajangsri, S.; Silvi, E.; Singh, T.; Andersson, P. G. Stereodivergent synthesis of trisubstituted enamides: direct access to both pure geometrical isomers. *J. Org. Chem.* **2019**, *84* (21), 13540−13548.

(18) (a) Nugent, T. C.; El-Shazly, M. Chiral amine synthesis-recent developments and trends for enamide reduction, reductive amination, and imine reduction. *Adv. Synth. Catal.* **2010**, *352* (5), 753−819. (b) Dewick, P. M. *Medicinal Natural Products: A Biosynthetic Approach*; John Wiley & Sons, 2002.

https://doi.org/10.1021/jacs.1c09573
J. Am. Chem. Soc. 2021, 143, 21594−21603